

ELASTIC PROPERTIES OF PERIODIC CORE'S STRUCTURES OF MULTILAYERS FURNITURE PANELS

M.Sc. Marlena WOJNOWSKA¹, M.Sc. Krzysztof PELIŃSKI¹, M.Sc. Michał MASLEJ¹,
Michał SŁONINA¹, Prof. Dr. Jerzy SMARDZEWSKI¹
marlene.stuefer@tum.de

¹Poznan University of Life Sciences, Faculty of Wood Technology, Department of Furniture
Design, 60-637 Poznan, ul. Wojska Polskiego 28

Abstract: The elastic properties of cellular structures of sandwich panel cores depend on their density. Density depends on a number of geometric parameters of the core structure. Research is ongoing to find optimal cell sizes with high stiffness of cores and low relative density. The aim of the investigation was to develop mathematical models describing the relative density and elastic properties of periodic cells: hexagonal, auxetic and lattice. Relative density models are presented as functions of main structural dimensions that affect the shape and size of individual cells. The analysis of the calculation results revealed that the relative density of the core cell was determined by: the thickness of the cell wall, the thickness of the rib, the angle of inclination of the walls and ribs, the length of the walls and the height of the core. For each of the cell types, three models were selected, with different geometries but with equal relative density. Additionally, linear elastic modulus was calculated, as well as modulus of elasticity and Poisson's coefficients for selected structures. Based on the above assumptions, reference cells with the highest mechanical parameters were selected.

Key Words: auxetic, density, mechanical properties, periodic cells, sandwich

1. GİRİŞ (INTRODUCTION)

Traditional honeycomb panels from wood-base materials are characterised by a relatively high strength and rigidity accompanied by small mass [1]. In particular, their high quality strength referred to their density is especially advantageous [2]. However, the main application problem is associated with the fact that wood-base honeycomb panels with paper cores cannot be used in elements less than 25 mm thick, the main reason being their low strength and stiffness in comparison with traditional panels [2-4]. However, the authors [5] quoted low production costs of panels more than 25 mm thick, which the furniture industry requires. In the paper [6], factors which need to be taken into consideration in production of honeycomb panels for furniture industry were discussed. These factors, for the hexagonal paper core, comprise: size of the mesh, height of filling, density of filling and cell orientation in relation to the panel sheet. In the case of facings, honeycomb panel rigidity depends on the stiffness along the longer axis of the element.

The performed experiments demonstrated that differences in panel rigidity and strength were due to variations in the relative density of cell cores. Moreover, it was confirmed [7] that property modification of these light structures can be achieved by interference in the shape of cell cores, their proportions, wall inclination angles as well as modification of the applied materials. The paper [2] indicates very limited availability of literature regarding modelling of mechanical properties associated with wood-base panel materials of honeycomb structure with cell cores. The author emphasises that panel material elasticity of honeycomb structure can be increased thanks to the auxetic nature of cell cores.

First researchers who described materials characterised by negative Poisson's coefficients were [8-10]. Multilayer composites having auxetic structures are characterised by increased: rigidity, elasticity [11, 12], buckling resistance [13], resistance to indentation and resistance to cracking [14-16] and ability to form synclastic shapes [2]. Value variations of Poisson's coefficient for the honeycomb panel are associated with changes in the cell geometry, whereas bending rigidity depends on the property of the material from which the core was manufactured [18]. Literature sources quoted above indicate the need to widen the scope of investigations from the area of materials with a layered sandwich type structure of auxetic nature. Features of auxetic materials predispose them to be used for production of structures with synclastic surfaces. In this regard, considerable studies were carried out on plastic materials or metal intended for a wide range of elements. On the other hand, few experiments were conducted regarding cores and facing layers manufactured from wood-base materials.

The objective of this study was to develop mathematical models describing relative density and elastic properties of the following periodic cells: hexagonal, auxetic, cylindrical and rib auxetic. Another cognitive objective of the performed experiments was to optimise the cell shape in the function of relative density minimization and maximization of linear elasticity moduli.

2. YÖNTEM (METHOD)

2.1. Mathematical models describing relative density and elastic properties of examined cells

For structures presented in Figures 1-4, the authors determined moduli of linear elasticity E_x , E_y , Poisson's coefficients ν_{xy} , ν_{yx} as well as the rigidity modulus G_{xy} . Calculation formulae were adopted after [19] and are presented in Tables 1-4. Cell relative density was determined as the ratio of the core density to the density of the substance constituting the skeleton of the structure. Below, mathematical models of the reference hexagonal cell as well as auxetic cells are presented.

2.1.1. Hexagonal cell

Figure 1 presents an elementary section of the honeycomb panel core with a hexagonally-shaped cell. The cell shape is determined by the following dimensions: l – length of the free side, h - length of the common side, t – wall thickness, L_x – cell length, S_y – cell width, f – wall inclination angle, e – inclination angle of the angle bisector between walls.

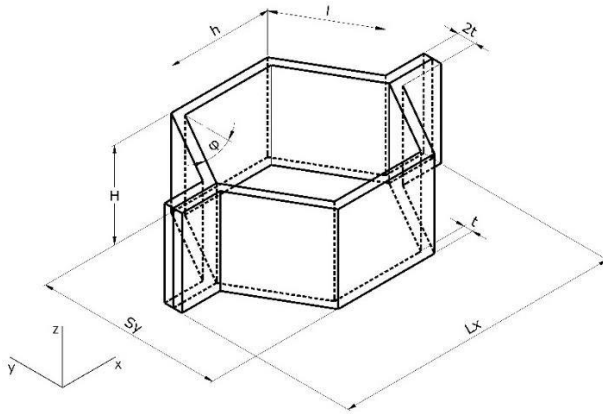


Figure 1. Elementary section of the core with hexagonal cells

Table 1. Mathematical models describing relative density and elastic properties of a hexagonal cell

Relative density	$\rho = 1 - \frac{l \cos(\varphi) (\sin(\varphi) (2l - t \tan(\varepsilon)) + 2h - 4t \tan(\varepsilon))}{2(l \sin(\varphi) + h - t \tan(\varepsilon))(t + l \cos(\varphi))}$	(1)
Modulus of linear elasticity E_x	$E_x = \frac{E_{st}^3 \left(\frac{h}{l} + \sin(\varphi)\right)}{l^3 \cos^3(\varphi)}$	(2)
Modulus of linear elasticity E_y	$E_y = \frac{E_{st}^3 \cos(\varphi)}{l^3 \left(\frac{h}{l} + \sin(\varphi)\right) \sin^2(\varphi)}$	(3)
Poisson's coefficient ν_{xy}	$\nu_{xy} = \frac{\sin(\varphi) \left(\frac{h}{l} + \sin(\varphi)\right)}{\cos^2(\varphi)}$	(4)
Poisson's coefficient ν_{yx}	$\nu_{yx} = \frac{\cos^2(\varphi)}{\left(\frac{h}{l} + \sin(\varphi)\right) \sin(\varphi)}$	(5)
Rigidity modulus G_{xy}	$G_{xy} = \frac{E t^3 \left(\frac{h}{l} + \sin(\varphi)\right)}{l^3 \left(\frac{h}{l} + \sin(\varphi)\right) \left(1 + \frac{2h}{l} \cos(\varphi)\right)}$	(6)

2.1.2. Bow-shaped auxetic cell

Figure 2 presents an elementary section of the honeycomb panel core with an auxetic bow-shaped cell. The cell shape is determined by the following dimensions: l_A - length of the free side, h_A - length of the common side, t_A - wall thickness, L_x - cell length, S_y - cell width, f_A - wall inclination angle, e_A - inclination angle of the angle bisector between walls.

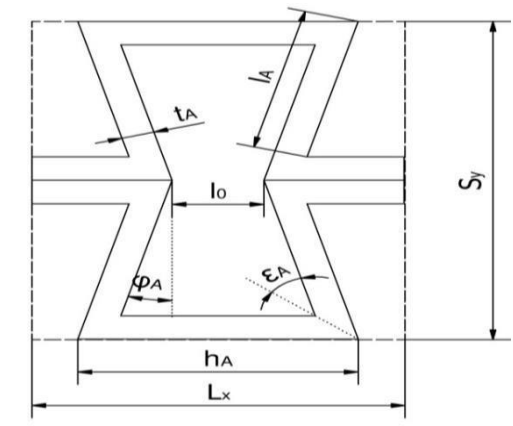


Figure 2. Elementary section of the core with an auxetic cell

Table 2. Mathematical models describing relative density and elastic properties of an auxetic cell

Relative density	$\rho = 1 - \frac{l \cos(\varphi) (\sin(\varphi) (2l - t \tan(\varepsilon)) + 2h - 4t \tan(\varepsilon))}{2(l \sin(\varphi) + h - t \tan(\varepsilon))(t + l \cos(\varphi))}$ (7)
Modulus of linear elasticity E_x	$E_x = \frac{K_f \cos(\varphi_A)}{b \left(\frac{h_A}{l_A} + \sin(\varphi_A) \right) \sin^2(\varphi_A)}$ (8)
Modulus of linear elasticity E_y	$E_y = \frac{K_f \left(\frac{h_A}{l_A} + \sin(\varphi_A) \right)}{H \cos^3(\varphi_A)}$ (9)
Poisson's coefficient ν_{xy}	$\nu_{xy} = \frac{\sin(\varphi_A) \left(\frac{h_A}{l_A} + \sin(\varphi_A) \right)}{\cos^2(\varphi_A)}$ (10)
Poisson's coefficient ν_{yx}	$\nu_{yx} = \frac{\left(\frac{h_A}{l_A} + \sin(\varphi_A) \right) \sin(\varphi_A)}{\cos^2(\varphi_A)}$ (11)
Rigidity modulus G_{xy}	$G_{xy} = \frac{K_f \left(\frac{h_A}{l_A} + \sin(\varphi_A) \right)}{H \left(\frac{h_A^2}{l_A^2} + 1 \right) \cos(\varphi_A)}$ (12)

2.1.3. Cylindrical cell

Analysing the geometry of the elementary section of the honeycomb panel core auxetic structure (Fig. 3), it should be noticed that it is made up of: cylindrical cells of R_1 external radius, R_2 internal radius and thickness of cell walls equalling $d = R_1 - R_2$. A ribbon of t thickness was placed between cylinders tangentially to their external surface. The shape of the applied ribbon made it possible to confer auxetic properties to the core structure.

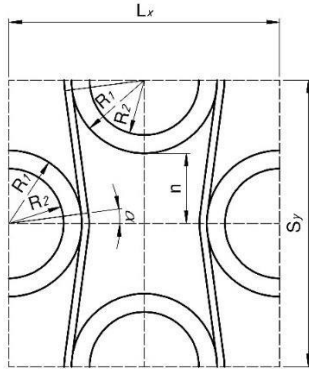


Figure 3. Elementary section of the auxetic core with cylindrical cells

Table 3. Mathematical models describing relative density and elastic properties of a cylindrical cell

Relative density	$\rho = \frac{\frac{1}{2} \pi (R_1^2 - R_2^2) + \frac{\varphi \pi}{180} ((R_1 + t)^2 - R_2^2) + 2tf}{(2R_2 + t - m)(R_1 + n)}$ (13)
Modulus of linear elasticity E_x	$E_x = \frac{E_s t^3 (2R_1 + t - m)}{f^3 (R_1 + n) \cos^2(\varphi)}$ (14)
Modulus of linear elasticity E_y	$E_y = \frac{E_s t^3 (R_1 + n)}{f^3 (2R_1 + t - m) \sin^2(\varphi)}$ (15)
Poisson's coefficient ν_{xy}	$\nu_{xy} = - \frac{t \tan(\varphi) (2R_1 + t - m)}{R_1 + n}$ (16)
Poisson's coefficient ν_{yx}	$\nu_{yx} = - \frac{ct \tan(\varphi) (R_1 + n)}{2R_1 + t - m}$ (17)

Rigidity modulus G_{xy}	$G_{xy} = \frac{E_s t^3 (2R_1 + t - m)}{2f^3 (R_1 + n - tg(\varphi)(2R_1 + t - m)) \cos^2(\varphi)} \quad (18)$
------------------------------	---

2.1.4. Auxetic rib cell

It should be noticed in the geometry of the 3D elementary structural section of the rib honeycomb core (Fig. 4) that it is made up of twelve identical pairs of arms inclined at angle f , where: L – length of the elementary cell section, l' – length of the projection of the cell arm, l – length of the cell arm, t – thickness of the node connecting the cell arms. In order to maintain technical feasibility of the cell, angle f should be contained within the interval $0^\circ < f < 40^\circ$. For reasons of symmetry, the auxetic cell of the 3D structure should exhibit identical elastic properties in all directions of the rectangular 3D coordinate system.

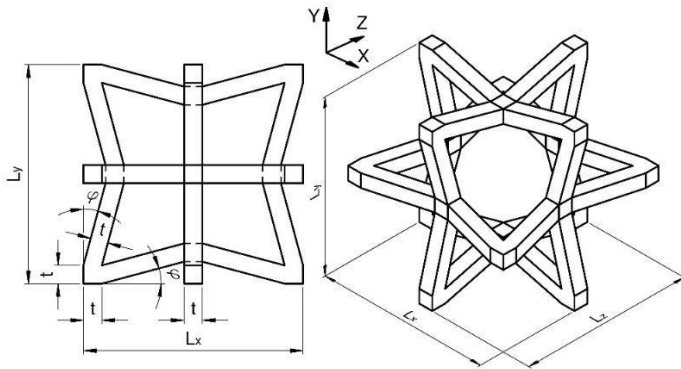


Figure 4. Elementary section of the structure of the rib auxetic core of a honeycomb panel

Table 4. Mathematical models describing relative density and elastic properties of an auxetic rib cell

Relative density	$\rho = \frac{V_s(ZX) + V_s(ZY)}{L_x L_y h} \quad (19)$
Linear elasticity modulus E	$E = \frac{E_s t^4 \cos^6(\varphi) (1 - tg(\varphi))^2}{(L_x - 3t)^3 (L_x - t) tg^2(\varphi) \sin(\varphi)} \quad (20)$
Poisson's coefficient ν	$\nu = -\cos(\varphi) \quad (21)$
Rigidity modulus G	$G = \frac{E}{2(1 - \nu)} \quad (22)$

2.2. Properties of auxetic cells

Bearing in mind the fact that cell density exerts a significant impact on the elastic properties of the core, the authors decided, in the further part of the study, to design the shape of an auxetic cell of relative density value similar to the density value of a reference hexagonal cell. For each of the type of cells, a reference hexagonal cell and three models of different geometry but identical relative density were collated. In addition, for selected structures, linear elasticity moduli as well as rigidity moduli and Poisson's coefficients were calculated. On the basis of the above assumptions, reference cells were collected of the highest mechanical parameters. From among hexagonal cells, the H1 cell seemed most regular and due to its more advantageous (higher) elastic properties, appeared more universal for core construction. Moreover, it exhibited lower anisotropy in comparison with the reference cell of H0 type. The H2 cell revealed strong variability of constant elastic values E_x, E_y as well as Poisson's coefficients ν_{xy}, ν_{yx} . The H3 cell

was characterised by the highest elasticity modulus E_x and the lowest modulus E_y , hence cell H3 was characterised by exceptionally strong orthotropy.

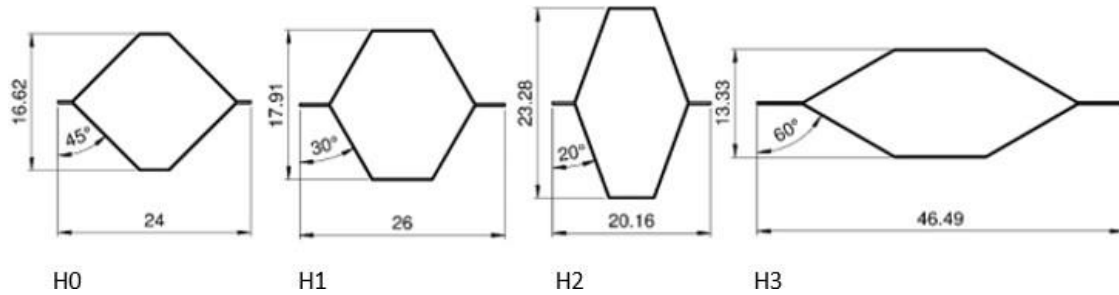


Figure 5. Geometry of selected core cells

Table 5. Characteristic properties of selected hexagonal cells (H0 – reference cell)

Cell type	E_x	t	h	l	f	L_x	S_y	r	E_x	E_y	u_{xy}	u_{yx}	G_{xy}
	MPa	mm			°	mm			MPa				MPa
H0	6000	0.15	3.9	11.5	45	23.99	16.62	0.02493	0.0389	0.0178	0.1017	1.48	0.68
H1	6000	0.15	8.0	10.2	30	25.99	17.91	0.02493	0.0381	0.0518	0.0179	0.86	1.17
H2	6000	0.15	6.0	12.2	20	20.15	23.28	0.02493	0.0111	0.1068	0.0206	0.32	3.10
H3	6000	0.15	12.0	13.0	60	46.48	13.33	0.02493	0.1308	0.0034	0.0136	6.19	0.16

Among bow-shaped auxetic cells, A3 and A1 cells qualified for further analyses. The first of the two was characterised by a very small value of the Poisson's coefficient u_{xy} and a high value of the modulus E_y as well as a small value of modulus E_x . However, this cell was fairly slender and may lead to technological problems. The A1 cell, at relatively high values of E_y and E_x moduli, was also characterised by satisfactory Poisson's coefficients in both directions and showed more regular geometry and side proportions along the X, Y axis and, consequently, exhibiting properties close to isotropic.

Table 6. Characteristic properties of selected auxetic cells (H0 – reference cell)

Cell type	E_x	t_A	h_A	l_A	f_A	L_x	S_y	r	E_x	E_y	u_{xy}	u_{yx}	G_{xy}
	MPa	mm			°	mm			MPa				MPa
A0	6000	0.15	3.9	11.5	45	23.99	16.62	0.0249	0.038	0.017	0.11	1.48	0.680
A1	6000	0.15	15.0	10.5	10	26.01	20.90	0.0249	0.023	0.458	-0.23	-4.43	0.002
A2	6000	0.15	20.0	10.6	25	30.57	19.51	0.0249	0.033	0.058	-0.75	-1.32	0.002
A3	6000	0.15	7.7	20.0	5	11.65	40.15	0.0249	0.000	1.109	-0.03	-38.0	0.003

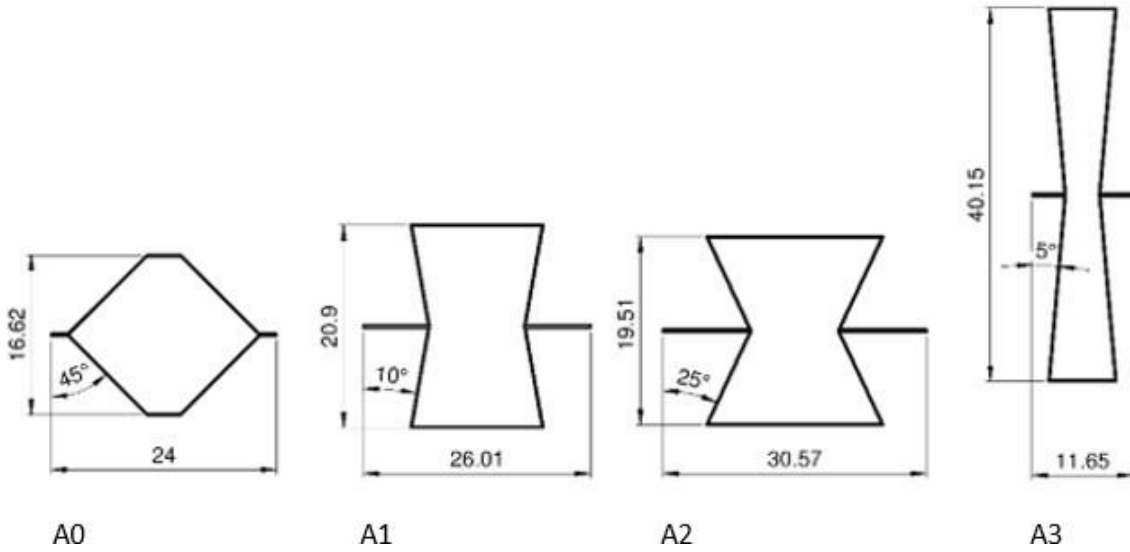


Figure 6. Geometry of selected core cells

In the case of cylindrical cells, increased dimensions of selected cells resulted in increased values of the inclination angle of the cell wall. It is also evident from Table 7, that increasing the value of the linear dimension along axis X resulted in increased linear elasticity modulus E_x , whereas increasing the S_y dimension – caused an increase of the E_y modulus. C2 cell is characterised by the most regular shape geometry. It also exhibited orthotropic properties. Cells whose external radius was below 10 mm exhibited higher values of the linear elasticity modulus E_y in relation to E_x ($E_y > E_x$). At the length of the radius R_1 exceeding 10 mm, cells exhibited reverse orthotropic properties $E_y < E_x$. Together with the increase of cell linear dimensions, the negative value of the Poisson's coefficient ν_{xy} also declined, in contrast to the Poisson's coefficient ν_{yx} .

Table 7. Characteristic properties of selected cylindrical cells (H0 – reference cell)

Cell type	E_s	m	n	Rl	f	L_x	S_y	r	E_x	E_y	ν_{xy}	ν_{yx}
	MPa	mm			°	mm			MPa			
C0	6000	2.0	7.0	5.0	11.974	16.3	24	0.04604	0.103	4.98	-0.144	-6.943
C1	6000	3.0	7.0	6.0	17.894	18.3	26	0.04585	0.117	2.26	-0.227	-4.400
C2	6000	5.0	5.1	10.0	45.854	30.3	30.2	0.04614	0.907	0.85	-1.034	-0.967
C3	6000	7.0	7.0	11.5	60.755	32.3	37	0.04662	1.078	0.44	-1.559	-0.641

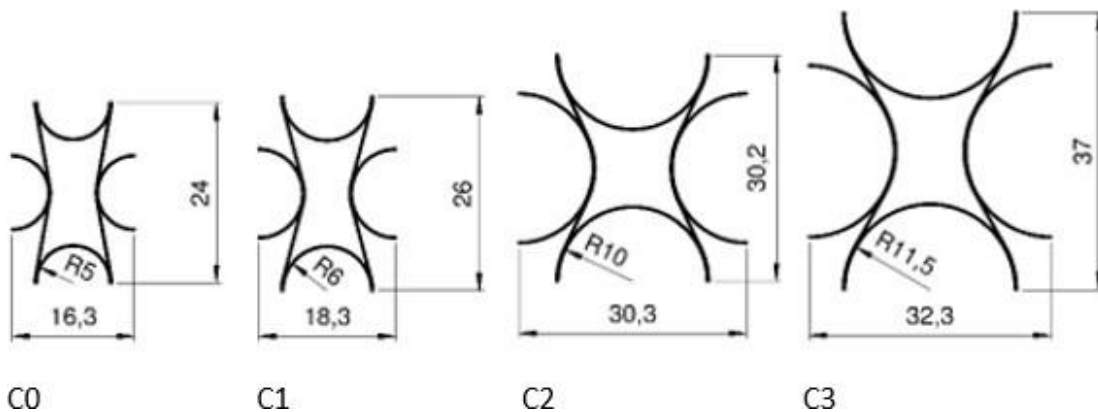


Figure 7. Geometry of selected core cells

Auxetic rib cells are characterised by a similar value of the Poisson's coefficient. The Z1 cell has the highest values of the moduli of linear elasticity E and rigidity G_{xy} . Also cell Z3 is characterised by advantageous elasticity properties. Cell Z2, whose elasticity moduli are close to 0, is characterised by properties most similar to the reference cell Z0.

Table 8. Characteristic properties of selected rib cells (Z0 – reference cell)

Cell type	E_s	t	h	f	L_x	r	E	ν	G_{xy}
	MPa	mm		°	mm		MPa		MPa
Z0	6000	0.50	12	45	6.3	0.02297	0.89	-0.906	0.23
Z1	6000	0.70	12	65	6.3	0.02311	1747.64	-0.999	437.21
Z2	6000	0.42	12	26	6.3	0.02165	0.03	-0.819	0.01
Z3	6000	0.70	14	70	7.25	0.02244	30.04	-0.978	7.59

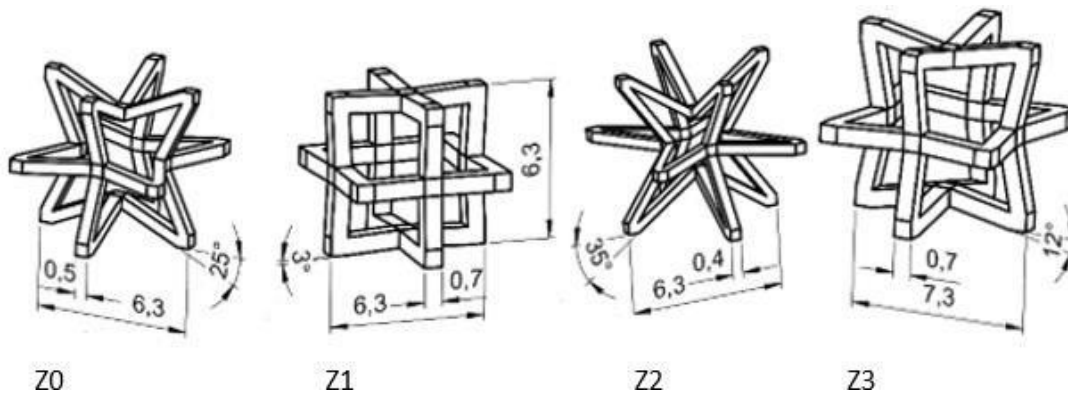


Figure 8. Geometry of selected core cells

2.3. Numerical optimisation of cell shape

When performing engineer calculations, it is recommended to apply statistical methods which constitute part of numerical methods of static optimisation [20-25]. In this context, methods of systematic search, random walk and Monte Carlo deserve attention. They consist in a systematic or random combing of the admissible region and, on the basis of the obtained results, estimation of the optimal value can be obtained. The optimisation object comprised cells of multilayer furniture panels with shapes presented in Figures 1-4. In this case, the authors adopted, as a natural optimisation criterion, minimisation of relative density and value maximisation of linear elasticity moduli of the elaborated core cells. Therefore, as the objective function, they assumed external dimensions of these cells as well as dimensions of individual cell walls. It should be remembered that reaching optimal solution must be preceded by a conjunctive fulfilment of numerous limiting conditions associated with cell shapes. The way in which to carry out the optimisation process was presented taking as an example a hexagonal reference cell.

The optimisation mathematical model of a polygonal auxetic cell comprised:

- a) decision variables for which cube of variables K_2 assumes the following shape:

$$K_2 = \{\bar{x} = (x_1 \dots x_4): x_{i(\min)} \leq x_i \leq x_{i(\max)}; i = 1 \dots 4\}.$$

where: i – number of decision variables for the cell; $x_1 = t$ thickness of the cell wall; $x_2 = h$ length of the common cell wall; $x_3 = l$ length of the free cell wall; $x_4 = f$ inclination angle of the cell wall,

- b) parameter E_s constituting the modulus of linear elasticity of the material from which cell walls were manufactured,
c) the acceptable set Φ is formed from inequality limits $\Phi_i(x) > 0$ i.e.:

$$\Phi = \{\bar{x} = (x_1 \dots x_4): \Phi_i(\bar{x}) > 0; i = 1 \dots 4\},$$

As the objective function, the authors adopted minimisation of the apparent cell density:

$$\rho = 1 - \frac{F_s}{F^*} \rightarrow \min,$$

and value maximisation of linear elasticity moduli in main directions of orthotropy:

$$E_x = \frac{E_s t^3 \cos^3(\varphi)}{l^3 \cos^3(\varphi)} \rightarrow \max,$$

$$E_y = \frac{E_s t^3 \cos(\varphi)}{l (l + \sin \varphi) \sin \varphi} \rightarrow \max.$$

Before initiation of the optimisation process, geometric parameters discussed earlier and presented in Figure 5 were collated. It was necessary to provide minimal, intuitively estimated, values of cell dimensions t_{\min} , h_{\min} , l_{\min} , f_{\min} as well as their maximum values t_{\max} , h_{\max} , l_{\max} , f_{\max} , which the authors intended to optimise. In the cube of decision variables, these values are described by extreme points D_{\min} , D_{\max} . In the course of the optimisation process, the computer picks randomly from a given cube any $D_i(t_i, h_i, l_i, f_i)$ points and remembers only these from among them which fulfil all limiting conditions. The point which describes the objective function best, represents the optimal (suboptimal) cell dimensions. Figure 9 presents the optimisation algorithm using the Monte-Carlo method.

The input data of the optimisation process comprised:

- $t_{\min} = 0.1$ mm,
- $t_{\max} = 3.0$ mm,
- $h_{\min} = 5$ mm,
- $h_{\max} = 20$ mm,
- $l_{\min} = 5$ mm,
- $l_{\max} = 20$ mm,
- $f_{\min} = 1^\circ$,
- $f_{\max} = 89^\circ$,
- $E_s = 6000$ MPa.

Setting the sampling number at $N_o = 30000$, which the computer should carry out in order to reach the optimal solution, random numbers are generated and selection of random points $D_i(t_i, h_i, l_i, f_i)$ from the cube area of decision variables is performed. The point determining the lowest value of the objective function after performing N_o samplings presents the optimal cell properties characterised by the lowest density and the highest values of linear elasticity moduli. It is worth mentioning that the process is considered as finished when the result following a huge number of samplings does not improve.

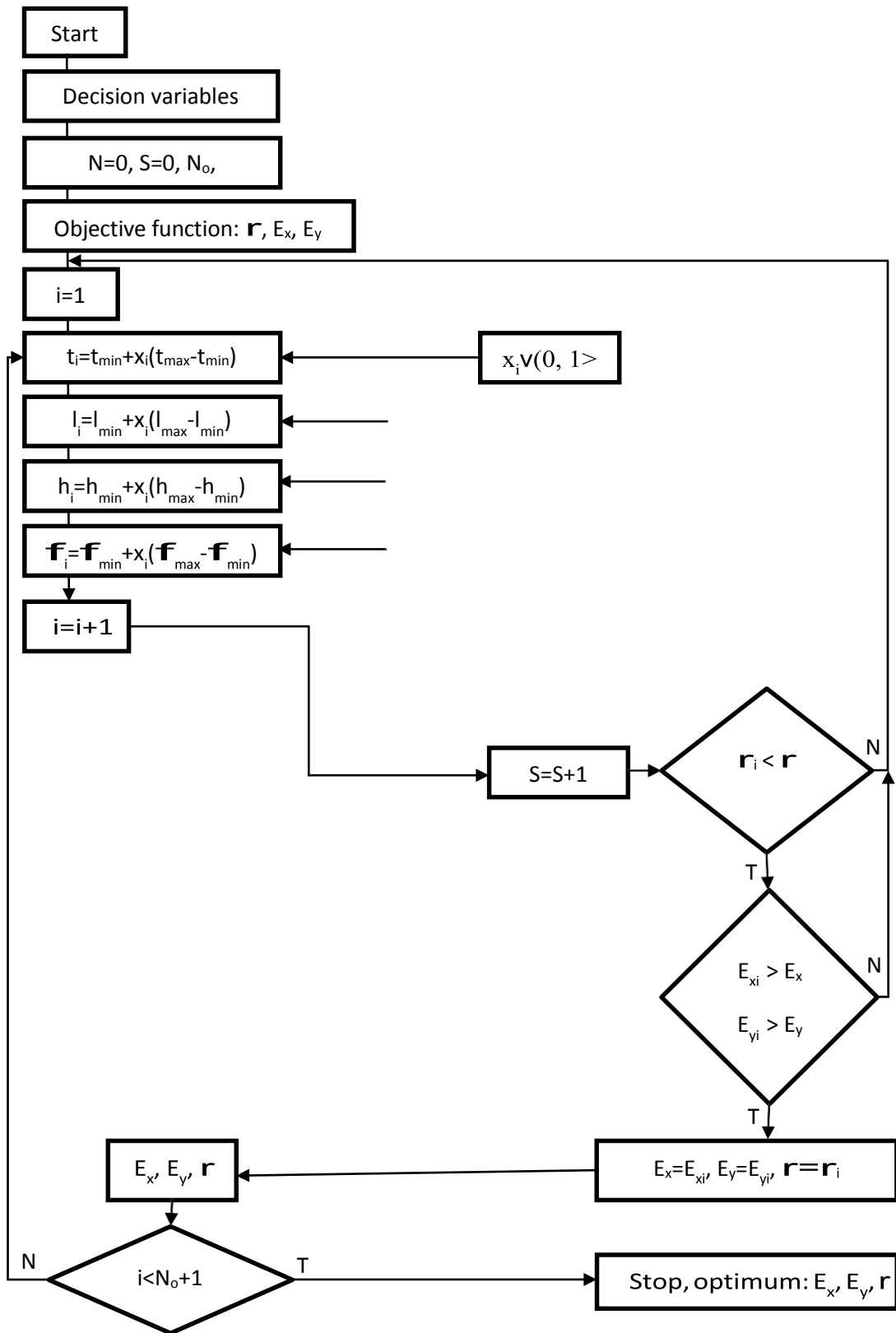


Figure 9. Optimisation algorithm of a hexagonal cell by the Monte-Carlo method

3. BULGULAR ((RESULTS) Research results and their analysis

Optimal cell properties with the smallest relative densities collated below were designated using D (density) index, while cells with the highest values of the linear elasticity moduli were marked with M (modulus) index.

3.1. Optimal cells

Characteristic properties of optimal hexagonal cells are presented in Table 9 and their shapes can be found in Figure 10, whereas information about optimal bow-shaped auxetic cells is to be found in Table 10 and Figure 11. Table 11 and Figure 12 present properties characteristic for optimal cylindrical cells, while Table 12 and Figure 13 - of auxetic rib cells.

Table 9. Characteristic properties of optimal hexagonal cells

Cell type	E_s	t	h	l	f	L_x	S_y	r	E_x	E_y	u_{xy}	u_{yx}	G_{xy}
	MPa	mm			°	mm			MPa				MPa
H_D	6000	0.10	14.9	19.6	33	51.01	33.01	0.00875	0.0017	0.0017	1.0133	0.99	0.00
H_M	6000	0.30	16.2	6.04	80	44.15	2.68	0.22260	503.78	0.0348	120.19	0.008	0.33

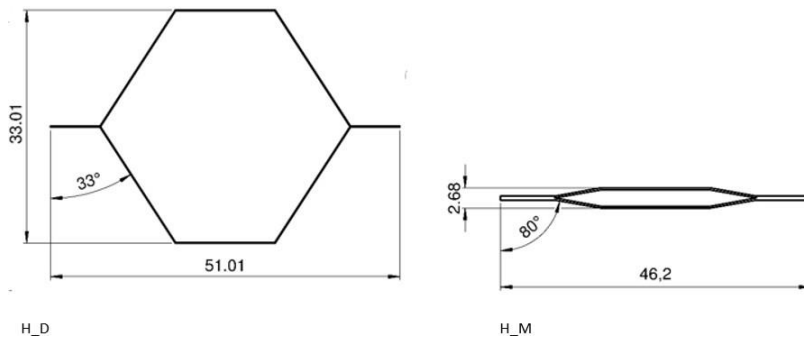


Figure 10. Geometry of core optimal hexagonal cells

Table 10. Characteristic properties of optimal bow-shaped auxetic cells

Cell type	E_s	t_A	h_A	l_A	f_A	L_x	S_y	r_A	E_x	E_y	u_{xy}	u_{yx}	G_{xy}
	MPa	mm			°	mm			MPa				MPa
A_D	6000	0.10	17.67	18.40	11.75	27.60	36.23	0.0116	0.0008	0.0329	-0.1608	-6.2206	0.0003
A_M	6000	0.66	19.49	5.42	10.26	35.47	13.9	0.1452	38.32	97.07	-0.6284	-1.5914	0.3505

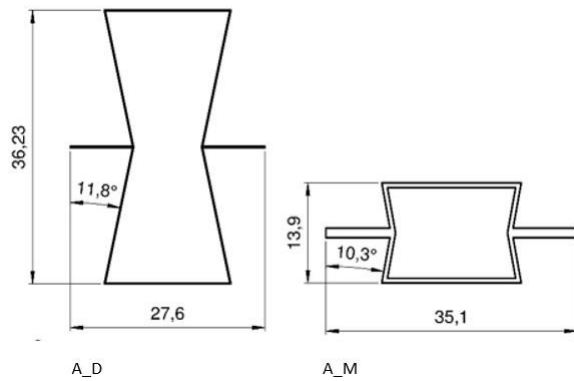


Figure 11. Geometry of core optimal auxetic cells

Table 11. Characteristic properties of optimal cylindrical auxetic cells

Cell type	E_x	m	n	RI	f	L_x	S_y	r	E_x	E_y	u_{xy}	u_{yx}	G_{xy}
	MPa	mm			°	mm			MPa				MPa
C_D	6000	2.1	6.6	12.0	7.68	44.1	37.3	0.01235	0.002	0.079	-0.159	-6.283	0.0012
C_M	6000	2.0	5.9	10.1	12.98	38.3	32.0	0.06899	23.93	314.46	-0.276	-3.625	16.526

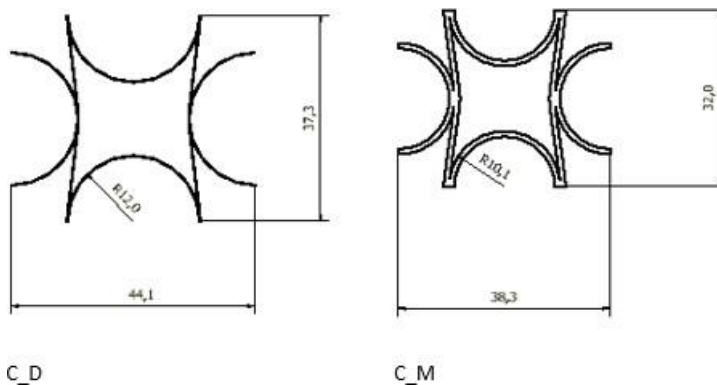


Figure 12. Geometry of core optimal cylindrical cells

Table 12. Characteristic properties of optimal rib auxetic cells

Cell type	E_x	t	f	L_x	r	E	u
	MPa	mm	°	mm		MPa	
Z_D	6000	0.30	3.032	7.25	0.00129	7.501	-0.9986
Z_M	6000	0.57	3.032	7.25	0.00843	81.36	-0.9986

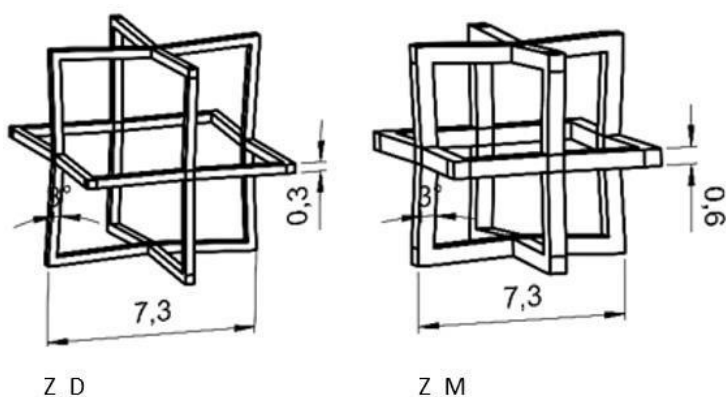


Figure 13. Geometry of core optimal rib auxetic cells

It is evident from the presented Figures and Tables that the H_M cell has three times thicker walls $t=0.3$ mm, three times shorter lengths of free walls $l=5.42$ mm, 2.44 times greater inclination angle of the cell wall $f=80$ and smaller overall dimensions ($L_x=44.15$ mm, $S_y=2.68$ mm) in relation to the H_D cell type with $L_x=51.01$ mm, $S_y=33.01$ mm dimensions. On the other hand, it is evident from Table 10 and Figure 11 that the A_M cell is characterised by six times thicker walls $t_A=0.66$ mm, three times shorter length of the free walls $l_A=5.42$ mm, a similar inclination angle of the cell wall $f_A=10.3^\circ$ and smaller overall dimensions ($L_x=35.47$ mm, $S_y=13.9$ mm) in relation to the auxetic cell of type A_D with $L_x=27.6$ mm, $S_y=36.23$ mm dimensions. Furthermore, it is clear from Table 11 and Figure 12 that the C_D cell possesses more than 18 times thinner walls and greater overall dimensions ($Rl=12$ mm, $L_x=44.1$ mm, $S_y=37.3$ mm) in relation to the C_M cell. However, this cell has greater linear elasticity moduli ($E_x=23.93$ MPa and $E_y=314.46$ MPa). On the other hand, it can be seen from Table 12 and Figure 13 that the Z_M cell is characterised by 90% thicker ribs and over 10 times greater linear elasticity modulus at the identical value of the inclination angle $f=3.032^\circ$ and identical linear dimension $L_x=7.25$ mm as the Z_D cell.

3.2. Coefficient of strength quality of optimal cells

For optimal cells with the highest values of linear elasticity moduli designated with M index, the authors calculated their strength quality coefficient as a relationship of E_x and E_y moduli to cell density (Fig. 14).

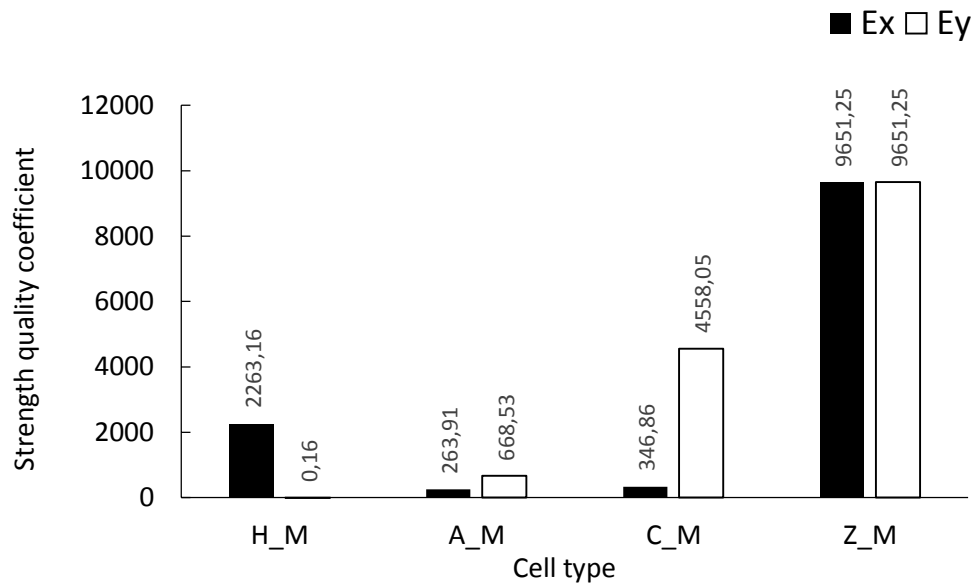


Figure 14. Coefficient of strength quality of optimal cells

The highest value of the strength quality coefficient was determined in the case of the rib auxetic cell (Z_M). This cell was characterised by isotropic properties. When analysing the relationship of the linear elasticity modulus E_x to relative density, the hexagonal cell H_M appeared advantageous. On the other hand, the cylindrical C_M cell seemed to be more advantageous from the point of view of the relationship of the linear elasticity modulus E_y to relative density.

4. SONUÇ VE TARTIŞMA (CONCLUSION)

On the basis of the performed analyses of results of analytical calculations, a number of conclusions were drawn and remarks made. Relative cell core density is determined by: the thickness of the cell wall, the inclination angle of walls and ribs, wall length and core height. It is not possible to obtain high cell linear elasticity moduli at a simultaneous lowest possible relative density. The Monte Carlo method of optimisation employed in this study made it possible to obtain optimal cell properties of possibly lowest density and maximum values of linear elasticity moduli. The highest values of strength quality were recorded in the case of rib auxetic cells.

The study was carried out within the framework of a research grant NCN OPUS 11 “Modelling of the properties of new lightweight wood-based honeycomb panels with auxetic cores”.

5. KAYNAKLAR (REFERENCES)

- [1] Jen Y, Chang L. Evaluating bending fatigue strength of aluminum honeycomb sandwich beams using local parameters. *Int J Fatigue* 2008;30:1103–14. doi:10.1016/j.ijfatigue.2007.08.006.
- [2] Smardzewski J. Elastic properties of cellular wood panels with hexagonal and auxetic cores. *Holzforschung* 2013;67:87–92. doi:10.1515/hf-2012-0055.
- [3] Smardzewski J. Mechanical properties of wood-based sandwich panels with a wavy core 2015.
- [4] Barboutis I, Vassiliou V. Strength Properties Of Lightweight Paper Honeycomb Panels For The Furniture. *10th Int Sci Conf Eng Des (Interior Furnit Des 2005:17–*

- 8.
- [5] J. Pflug, Vangrimde B, Verpoest I, Vandepitte D, Britzke M, Wagenführ A. Continuously Produced Paper Honeycomb Sandwich Panels for Furniture Applications. 5th Glob Wood Nat Fibre Compos Symposium 2004:1–9.
 - [6] Sam-brew S, Semple K, Smith GD. Preliminary Experiments on the Manufacture of Hollow Core Composite Panels. For Prod J 2011;61:381–9.
 - [7] Hu L, You F, Yu T. Effect of cell-wall angle on the in-plane crushing behaviour of hexagonal honeycombs. Mater Des 2013;46:511–23. doi:10.1016/j.matdes.2012.10.050.
 - [8] RS L. Foam Structures with a Negative Poisson's Ratio 1987.
 - [9] Gibson L. AM. Cellular solids: structure and properties 1988.
 - [10] Evans KE. Design of doubly curved sandwich panels with honeycomb cores 1991:95–111.
 - [11] Caddock B., Evans K. MI. Honeycomb cores with a negative Poisson ' s ratio for use in composite sandwich panels 1991.
 - [12] Masters 1. EK. Auxetic honeycombs for composite sandwich panels 1993:1–2.
 - [13] Miller W, Smith CW, Scarpa F, Evans KE. Flatwise buckling optimization of hexachiral and tetrachiral honeycombs. Compos Sci Technol 2010;70:1049–56. doi:10.1016/j.compscitech.2009.10.022.
 - [14] Scarpa F. TP. On the transverse shear modulus of negative Poisson's ratio honeycomb structures 2000.
 - [15] Evans K. AA. Auxetic Materials: Functional Materials and Structures from Lateral Thinking! 2000.
 - [16] Yang W., Li Z.-M., Shi W., Xie B.—H. YM —B. Review on auxetic materials 2004:8.
 - [17] T L. Flexural Rigidity Of Thin Auxetic Plates n.d.:1–6.
 - [18] Gibson L., Ashby M., Schajer G. RC. The Mechanics of Two-Dimensional Cellular Materials 1982.
 - [19] Masters IG, Evans KE. Models for the elastic deformation of honeycombs. Compos Struct 1996;35:403–22. doi:10.1016/S0263-8223(96)00054-2.
 - [20] Dziuba T. Optimierung der Konstruktion von Stuhlseitenteilen. Holztechnologie 30, 6: 303–306. 1990.
 - [21] Goliński J. Metody optymalizacyjne w projektowaniu technicznym (Optimisation methods in technical designing). Wydawnictwo Naukowo-Techniczne, Warszawa. 1974.
 - [22] Ostwald H. Optymalizacja konstrukcji (Construaction optimisation). Wydawnictwo Politechniki Poznańskiej, Poznań. 1987.
 - [23] Smardzewski J. Optymalizacja konstrukcji skrzydeł okiennych (Construction optimisation of window wings). Przemysł Drzewny, 4: 21–24. 1989.
 - [24] Smardzewski J. Numeryczna optymalizacja konstrukcji krzeseł (Numerical optimisation of chair constructions). Przemysł Drzewny, 1: 1–6. 1992.
 - [25] Jerzy Smardzewski. Furniture Design. Springer. 2015.